

Indoor Experiments of Real-Time MU-MIMO with CSI Feedback Scheme for Wireless LAN Systems

Koichi Ishihara, Yusuke Asai, Riichi Kudo, Takeo Ichikawa and Masato Mizoguchi
NTT Network Innovation Laboratories, NTT Corporation, Yokosuka, Japan
E-mail: ishihara.koichi@lab.ntt.co.jp

Abstract— This paper presents indoor experimental results on an implemented real-time downlink multiuser multiple-input multiple-output (DL-MU-MIMO) transceiver with a channel state information (CSI) feedback scheme for next generation wireless LAN systems. Estimated CSI is used at the access point (AP) transmitter to calculate transmit beamforming weight for DL-MU-MIMO transmission. A CSI compression scheme using discrete cosine transform (DCT) is proposed to reduce CSI feedback overhead. The transceiver performance is demonstrated and indoor experiments clarify that it is a feasible tool for real-time signal processing that improves system throughput over that of transceiver without a CSI compression scheme with simple digital signal processing of single-antenna stations (STAs).

Keywords—component; multiuser MIMO; CSI feedback, OFDM; downlink; wireless LAN

I. INTRODUCTION

In wireless communication systems, the multiuser multiple-input multiple-output (MU-MIMO) technique is an attractive candidate to improve spectrum efficiency especially when the number of antenna branches at the stations (STAs) is less than that at the access point (AP) [1]. Although the channel capacity of single-user MIMO is confined to the number of antennas at the STA, multiple STAs generate a large virtual array antenna so that a high spatial diversity effect is expected even when using simple STAs. There have been many studies pertaining to MU-MIMO systems, e.g., [2]–[4]. In already deployed wireless access systems, orthogonal frequency division multiplexing (OFDM) is adopted to mitigate the effect of multipath fading channels, and a combination of the MIMO and OFDM techniques is employed in the latest wireless access standards such as IEEE 802.11n [5]. The MIMO technique can be employed on a subcarrier basis, which makes it possible to reduce the calculation complexity of the signal processing. Therefore, MU-MIMO-OFDM promises to greatly increase the channel capacity in a frequency-selective environment. The next generation wireless LAN system with a target data transfer rate of more than 1-Gbit/s is studied in IEEE 802.11ac and downlink (DL-)MU-MIMO-OFDM has been extensively investigated to improve the spectrum efficiency [6]. We have previously considered some elemental DL-MU-MIMO-OFDM technologies and presented their effectiveness [7], [8].

In DL-MU-MIMO, accurate estimate of channel state information (CSI) between an AP and each STA is required to perform transmit beamforming at the AP. In general, there are two CSI feedback schemes for transmit beamforming: *explicit feedback* and *implicit feedback*. For the former in particular, the amount of CSI is expected to increase since the numbers of transmitter and receiver antennas, subcarriers, and STAs become larger for higher data transmission. Furthermore, MU-MIMO transmission requires more accurate estimate of CSI than single-user MIMO transmission although it is necessary for achieving higher MAC efficiency to reduce CSI feedback duration. To address this problem, many CSI feedback schemes have been proposed, e.g., in [9]–[13]. A time-domain approach is particularly effective in reducing the amount of feedback information, as we demonstrated with a proposed time-domain CSI feedback scheme using discrete cosine transform (DCT) for DL-MU-MIMO [13]. Although channel estimation schemes using DCT have been proposed in [14], [15], we proposed applying them to CSI feedback, using DCT to obtain the impulse response of the CSI estimate. We assumed that the number of coefficients of the actual channel impulse response is fewer than that of subcarriers since CSI in the time domain consists of fewer than N_c (N_c being the number of cyclic prefix (CP) samples) components even though in the frequency domain it consists of N_{sc} subcarrier components, and that consequently less CSI feedback is needed with impulse response than with subcarriers.

This paper presents an implemented real-time DL-MU-MIMO-OFDM transceiver with a DCT-based CSI feedback scheme using a field programmable gate array (FPGA). In the transceiver, CSI is estimated at each STA. The STAs feed it back to an AP using the proposed CSI feedback scheme. At the AP, zero forcing (ZF) beamforming weight is calculated using the CSI and DL-MU-MIMO transmission is then carried out in real-time digital signal processing. In this paper, we describe experimental results obtained with the transceiver in an actual indoor environment and show that DL-MU-MIMO transmission with the proposed CSI feedback scheme can achieve high throughput transmission even with single-antenna STAs.

The remainder of this paper is organized as follows. We first explain the configuration of the transceiver in Section II. Section III describes the CSI feedback scheme. In Section IV, we present indoor experimental results we obtained with it that confirm its effectiveness. Section V concludes the paper with a brief summary of key points.

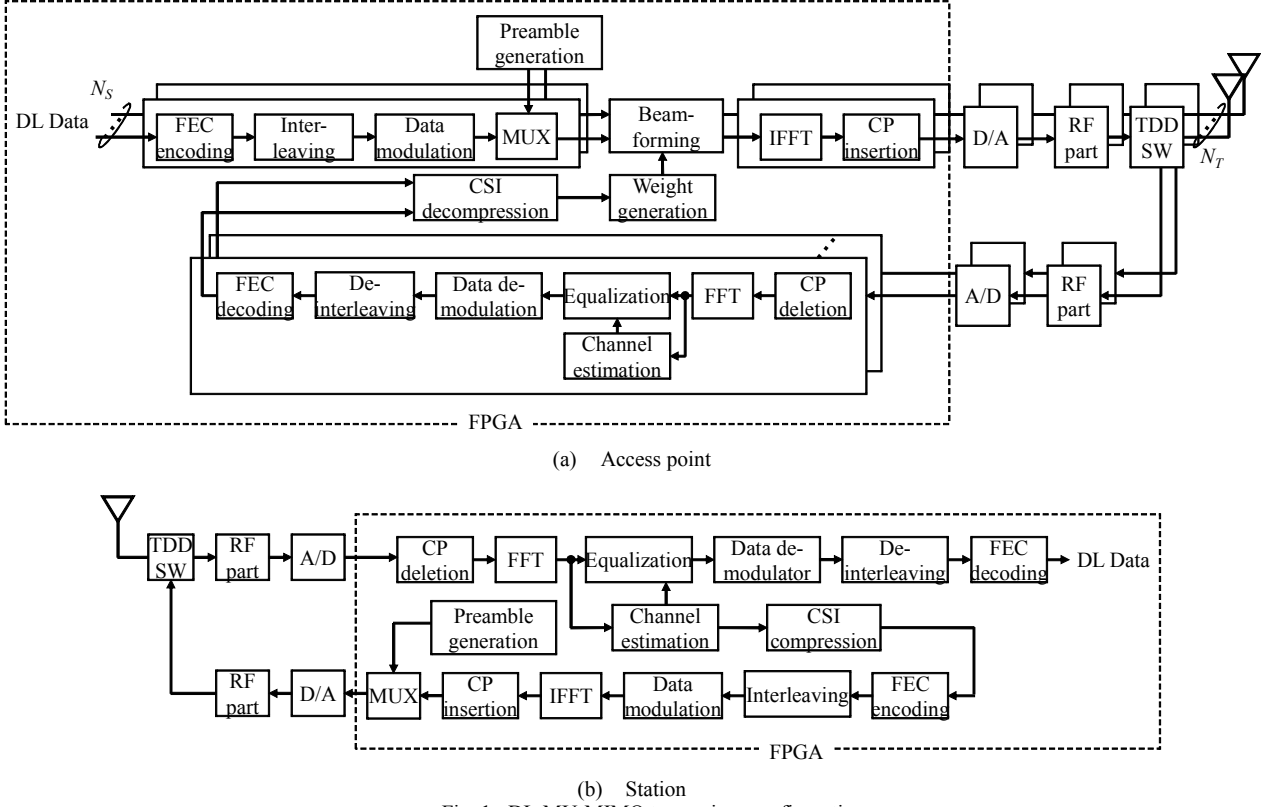


Fig. 1 DL-MU-MIMO transceiver configuration.

II. DL-MU-MIMO TRANSCEIVER CONFIGURATION

Figure 1 shows the DL-MU-MIMO transceiver configuration. The major transceiver parameters are listed in Table I. The carrier frequency is 4.85 GHz and the maximum number of STAs for DL-MU-MIMO transmission is six. The number of subcarriers is 228, which includes 12 pilot subcarriers and is divided into four groups. Data frame length is 2.37 ms and frames consist of 8 subframes. At the AP transmitter, six-antenna OFDM signals with transmit bandwidth of 80 MHz are generated. At the STA receiver, the signals from the AP are received at an antenna. Channel coding is convolutional coding. Digital signal processing at both AP and STAs is implemented in FPGA.

Figure 2 shows the transceiver's frame sequence structure. The structure consists of a sounding frame, CSI feedback (CSI-FB) frames, and a data frame. At the AP, the sounding frame is first transmitted to STAs. Figure 3 shows the sounding frame structure. The frame consists of a short preamble and a long preamble. Both preambles are constructed from the 40 MHz version of IEEE 802.11n [16] by duplicating and frequency shifting. Moreover, the long preamble uses an 8-by-8 Hadamard matrix [17] and six OFDM symbols are transmitted to estimate the 6-by-1 CSI vector between the six transmit antennas at the AP and an antenna at each STA.

At each STA, the CSI vectors are estimated using the received sounding frame at each subcarrier. Each CSI estimate is then compressed using the proposed CSI feedback scheme,

which will be described in Sect. III. The compressed CSI is encoded using convolutional coding. After interleaving and data modulation mapping, the data symbol sequence is converted into an OFDM signal with 228 subcarriers using 256-point inverse fast Fourier transform (IFFT). OFDM-modulated CSI is then transmitted with short and long preambles to the AP as a CSI-FB frame. Here, in uplink transmission, a CSI-FB frame is transmitted from each STA in a time division multiple access (TDMA) manner.

After receiving the CSI-FB frame, the obtained compressed-CSI is decompressed using the proposed scheme and CSI of each subcarrier is obtained at the AP. The transmit beamforming weight based on ZF is then computed at each subcarrier at the AP for DL-MU-MIMO transmission. After computing the beamforming weight, the transmitted DL-MU-MIMO signal is generated. First, a data sequence is encoded using convolutional coding and interleaving is carried out for each STA. After data modulation and pilot (short and long preambles) insertion, the transmit beamforming is performed in both the data and pilot sequence using the computed weight at each subcarrier. Figure 4 shows the data subframe structure. As the figure shows, the subframe's long preamble consists of $2N_s$ OFDM symbols, where N_s is the number of STAs. The transmit beamforming for each STA is performed in each OFDM symbol to obtain an interference-free CSI estimate at each STA. The 256-point IFFT is then applied to produce the time-domain OFDM symbol for each transmitted stream. After CP insertion, DL-MU-MIMO signal sequences are transmitted from six antennas at the AP.

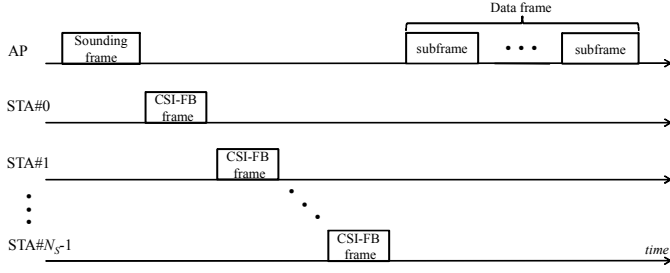


Fig. 2. Frame sequence structure.

At the STA, channel estimation is carried out using the long preamble at each subcarrier. The received data signals are equalized and demodulated using the channel estimates. After data demodulation, channel decoding is carried out using Viterbi decoding. Here, in our implemented DL-MU-MIMO transceiver, simple decoding can be carried out as in SISO transmission at each STA. This is because ZF transmit beamforming can provide orthogonal transmission between each stream ideally and each STA can simply decode the received signal even with a single antenna.

TABLE I. MAJOR DL-MU-MIMO TRANSCEIVER PARAMETERS

Bandwidth	80 MHz
Carrier frequency	4.85 GHz
Number of antennas	6 (AP) / 1 (STA)
Number of STAs	4
Maximum total transmit power	30 dBm
Number of subcarriers	228 (w/ 12 pilot subcarriers)
OFDM symbol duration	4.0 μ s (3.2 μ s + CP 0.8 μ s)
Data subframe length	296 μ s
Data frame length	2.37 ms (8 data subframes)
Data modulation	64QAM
Channel coding/decoding	Convolutional coding ($R=1/2$)/Viterbi decoding

III. CSI FEEDBACK SCHEME

At each STA, CSI is estimated using the long preamble of the sounding frame transmitted from the AP at each subcarrier. The channel impulse response is then obtained by applying DCT to the CSI estimate as follows:

$$h(l, n, m) = W(l) \sum_{k=0}^{K-1} H(k, n, m) \cos\left(\frac{\pi(2k+1)l}{2K}\right), \quad (1)$$

where

$$W(l) = \begin{cases} \sqrt{\frac{1}{K}}, & l=0 \\ \sqrt{\frac{2}{K}}, & l \neq 0 \end{cases}. \quad (2)$$

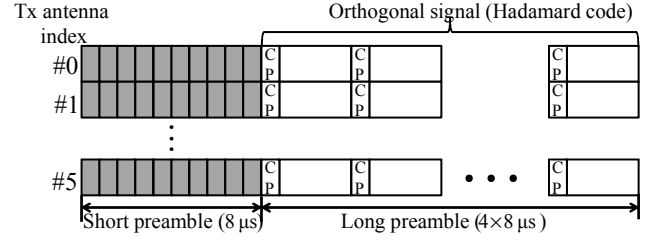


Fig. 3. Sounding frame structure.

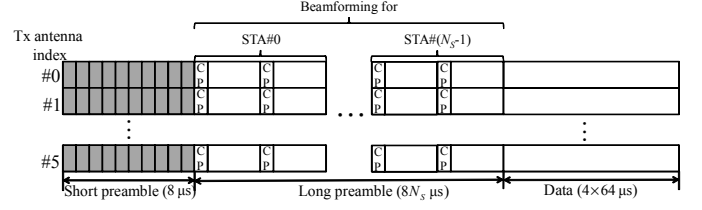


Fig. 4. Data subframe structure.

$H(k, n, m)$ is the channel gain estimate for the $k(=0, \dots, K-1)$ -th subcarrier between the $m(=0, \dots, N_T-1)$ -th transmit antenna at the AP and the $n(=0, \dots, N_S-1)$ -th STA. K is the number of DCT points. Here, most of the impulse response energy of the actual CSI concentrates not within all the samples in the DCT block but in some of the beginning samples, since the CSI's actual impulse response exists within N_c samples [14]. Assuming that the actual channel impulse response is present only within the beginning L samples, we consider that the beginning L elements $\{h(l, n, m), 0 \leq l \leq L-1\}$ of the channel impulse response are fed back to the AP. As shown in 11n [16], the coefficients of L elements are then normalized as

$$\hat{h}(l, n, m) = \frac{10^{\frac{Y(l, n)}{5}} h(l, n, m)}{\max_l(z(l, n))}, \quad (3)$$

where

$$z(l, n) = \max_m \left(\max \left(|\operatorname{Re}(\hat{h}(l, n, m))|, \max \left(|\operatorname{Im}(\hat{h}(l, n, m))| \right) \right) \right) \quad (4)$$

$$Y(l, n) = \min \left(2^{b_1} - 1, \left\lfloor 5 \log_{10} \left(\frac{\max_l(z(l, n))}{z(l, n)} \right) \right\rfloor \right), \quad (5)$$

and $\lfloor x \rfloor$ is the largest integer smaller than or equal to x . The real and imaginary parts of $\hat{h}(l, n, m)$ are then quantized to b_0 bits. Each STA sends the quantized $\operatorname{Re}[\hat{h}(l, n, m)]$ and $\operatorname{Im}[\hat{h}(l, n, m)]$ and the normalization factor $Y(l, n)$ of b_1 bits to the AP as the feedback information in CSI-FB duration.

At the AP, the normalized samples $\operatorname{Re}[\hat{h}(l, n, m)]$ and $\operatorname{Im}[\hat{h}(l, n, m)]$ are restored using the normalization factor as

$$h(l, n, m) = 10^{-\frac{Y(l, n)}{5}} \hat{h}(l, n, m). \quad (6)$$

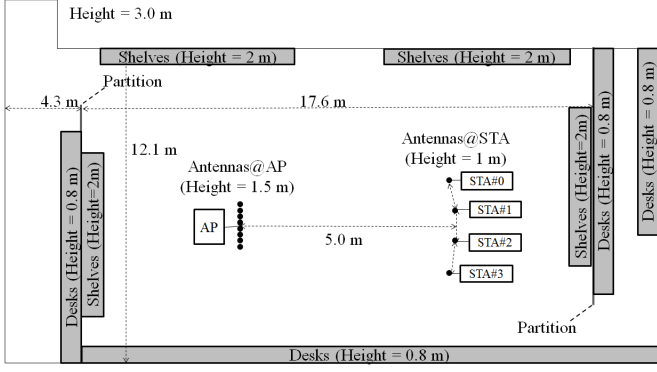


Fig. 5. Indoor measurement environment.

Inverse DCT (IDCT) is then applied to obtain K subcarrier components of the CSI.

$$\tilde{H}(k, n, m) = \sum_{l=0}^{L-1} W(l) h(l, n, m) \cos\left(\frac{\pi(2k+1)l}{2K}\right) \quad (7)$$

Finally, ZF weight [18] for transmit beamforming is generated using obtained CSI at each subcarrier as

$$\mathbf{W}(k) = \mathbf{H}(k)^H (\mathbf{H}(k) \mathbf{H}(k)^H)^{-1}, \quad (8)$$

where

$$\mathbf{H}(k) = \begin{bmatrix} \tilde{H}(k, 0, 0) & \cdots & \tilde{H}(k, 0, N_T - 1) \\ \vdots & \ddots & \vdots \\ \tilde{H}(k, N_S - 1, 0) & \cdots & \tilde{H}(k, N_S - 1, N_T - 1) \end{bmatrix}, \quad (9)$$

and $\mathbf{H}(k)^H$ stands for the conjugate transpose of $\mathbf{H}(k)$. Note that the proposed scheme must apply DCT to each group of consecutive subcarriers since discontinuity due to null subcarrier results in a spreading of energy. In the implemented transceiver, the subcarriers are divided into four groups. Therefore, the proposed scheme can reduce the amount of feedback information needed by the conventional one, where frequency-domain CSI is fed back by a factor of $4L/N_{sc}$.

IV. EXPERIMENTAL RESULTS

Figure 5 shows the indoor measurement environment. The AP antenna arrays had an element spacing of 0.06 m ($\approx 1.0\lambda$, where λ is the wavelength). We used linear arrays with six antennas at the AP. The distance between adjacent STAs is 2.0 m . The antenna heights at the AP and the STAs were 1.5 m and 1.0 m , respectively. The total maximum transmit power was 30 dBm . 64QAM was applied to all streams (or STAs) and the coding rate was set at $R=1/2$. The parameter for quantization was set to $(b_0, b_1)=(8,3)$. In these measurements, the STA locations were slightly moved to obtain the average value of throughput. In this experiment, CSI-FB uplink frames were

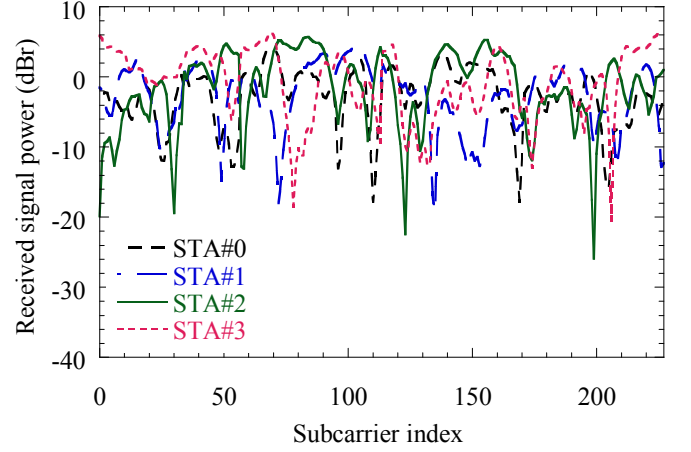


Fig. 6. Measured instantaneous signal power of each subcarrier.

transmitted through wired transmission in TDMA manner and there is no propagation error in CSI feedback.

Figure 6 shows an example of the measured instantaneous signal power of each subcarrier over 228 subcarriers between a transmit antenna at the AP and four STAs with an 80-MHz bandwidth. The vertical axis is the signal power normalized by average signal power when total transmit power from transmit antennas is 16 dBm . The figure clearly shows that the received signal power over 228 subcarriers varies over a wide range of nearly 30 dB , which results in frequency-selective fading channel with severe fading in spite of the line-of-sight (LOS) environment. Furthermore, it is seen that there is almost no correlation between the channel gains of each STA.

Figure 7 shows the average throughput performance of each STA with the feedback elements L as parameters. When the number of feedback elements of the channel impulse response L becomes small, the amount of feedback information bits can be reduced. However, throughput performance with $L=16$ significantly degrades since the amount of feedback information is not sufficiently high to produce the transmit beamforming and consequently inter-user interference occurs. In the next experiments, $L=24$ is used for the proposed CSI feedback scheme.

Finally, figure 8 plots the average throughput performance as a function of our DL-MU-MIMO transceiver's average total transmit power at the AP. For comparison, it also plots the average throughput performance for a transceiver without a CSI compression scheme, where the number of feedback information bits for CSI $\text{Re}[H(k, n, m)]$ or $\text{Im}[H(k, n, m)]$ is 12. As the figure shows, when the average transmit power is less than 10 dBm , the throughput performance with the proposed CSI feedback scheme is degraded by about 1 dB compared to that without a CSI compression scheme due to CSI error. However, when the transmit power is more than 10 dBm , the throughput performance with the proposed scheme is 10% better than that without a CSI compression scheme and a throughput value of over 100 Mbit/s is achieved because of the reduction of the CSI feedback duration.

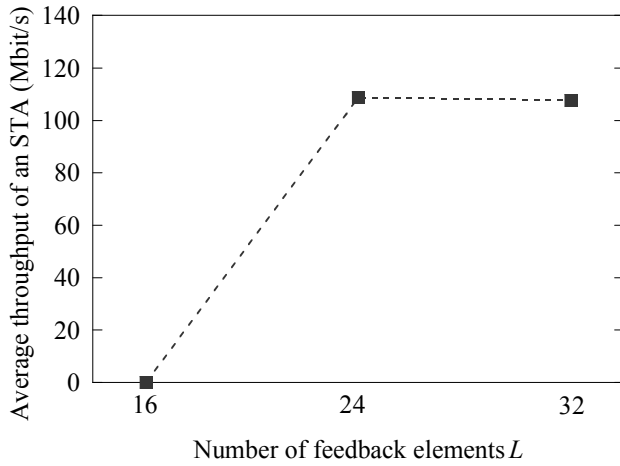


Fig. 7. Effect of feedback elements L .

V. CONCLUSION

This paper presents indoor experimental results on real-time DL-MU-MIMO transmission in an implemented DL-MU-MIMO transceiver with a CSI feedback scheme for next generation wireless LAN systems. The experiment results showed that real-time DL-MU-MIMO transmission was achieved using the proposed CSI feedback scheme. In the transceiver, CSI is compressed using DCT and the amount of feedback information of the CSI is compressed. The experimental results confirm that the proposed CSI feedback scheme can be practically applied to real-time signal processing hardware.

REFERENCES

- [1] A. Goldsmith, S. A. Jafar, N. Jindal, and S. Vishwanath, "Capacity limits of MIMO channels," *IEEE JSAC*, vol. 21, no. 5, pp. 684-702, June 2003.
- [2] Q. H. Spencer, A. L. Swindlehurst, and M. Haardt, "Zero-forcing methods for downlink spatial multiplexing in multiuser MIMO channels," *IEEE Trans. Signal Processing*, vol. 52, pp. 461-471, Feb. 2004.
- [3] L. U. Choi and R. D. Murch, "A transmit preprocessing technique for multiuser MIMO systems using a decomposition approach," *IEEE Trans. Wireless Commun.*, vol. 3, pp. 653-668, Jan. 2004.
- [4] Z. Shen, R. Chen, J. G. Andrews, R. W. Heath, Jr. and B. L. Evans, "Low complexity user selection algorithms for multiuser MIMO systems with block diagonalization," *IEEE Trans. Signal Processing*, vol. 54, no. 9, Sep. 2006.
- [5] E. Perahia, "IEEE 802.11n development: history, process, and technology," *IEEE Commun. Mag.*, vol. 46, no. 7, pp. 48-55, July 2008.
- [6] R. Stacey, "Proposed specification framework for TGac," *IEEE802.11-09/992r19*, Jan. 2011.
- [7] K. Nishimori, R. Kudo, Y. Takatori, A. Ohta, and K. Tsunekawa, "Performance evaluation of 8x8 multi-user MIMO-OFDM testbed in an actual indoor environment," in *Proc. PIMRC*, Sep. 2006.
- [8] R. Kudo, Y. Takatori, K. Nishimori, A. Ohta, and S. Kubota, "User selection method for block diagonalization in multiuser MIMO systems," in *Proc. IEEE GLOBECOM*, Nov. 2007.
- [9] D. J. Love, R. W. Heath Jr., W. Santipach, and M. L. Honig, "What is the value of limited feedback for MIMO channels?," *IEEE Commun. Mag.*, vol. 42, no. 10, pp. 54-59, Oct. 2004.
- [10] N. Jindal, "MIMO broadcast channels with finite-rate feedback," *IEEE Trans. Inf. Theory*, vol. 52, no. 11, pp. 5045-5060, Nov. 2006.
- [11] H. S. Mehr, and G. Caire, "Channel state feedback schemes for multiuser MIMO-OFDM downlink," *IEEE Trans. Commun.*, vol. 57, no. 9, Sep. 2009.
- [12] Y. Su, S. Tang, J. Shi, X. Huang, and Y. J. Guo, "Robust downlink precoding in multiuser MIMO-OFDM systems with time-domain quantized feedback," in *Proc. IEEE WCNC*, Apr. 2010.
- [13] K. Ishihara, Y. Takatori, Y. Asai, R. Kudo, and M. Mizoguchi, "CSI feedback methods for downlink MU-MIMO in WLANs," in *Proc. Asia-Pacific Radio Science Conf.*, Sep. 2010.
- [14] H. Kobayashi, and K. Mori, "Proposal of OFDM channel estimation method using discrete cosine transform," in *Proc. PIMRC*, vol. 3, pp. 1797-1801, Sep. 2004.
- [15] M. Diallo, R. Rabineau, L. Cariou, and M. Helard, "On improved DCT based channel estimation with very low complexity for MIMO-OFDM systems," in *Proc. IEEE VTC-spring*, Apr. 2009.
- [16] Wireless LAN medium access control (MAC) and physical layer (PHY) specifications: Enhancements for higher throughput, *IEEE Standard 802.11n*, 2009.
- [17] J. G. Proakis, *Digital communications*, Fourth edition, McGraw-Hill, 2001.
- [18] M. Joham, W. Utschick, and J. A. Nossek, "Linear transmit processing in MIMO communications systems," *IEEE Trans. Signal processing*, vol. 53, no. 8, pp. 2700-2712, Aug. 2005.

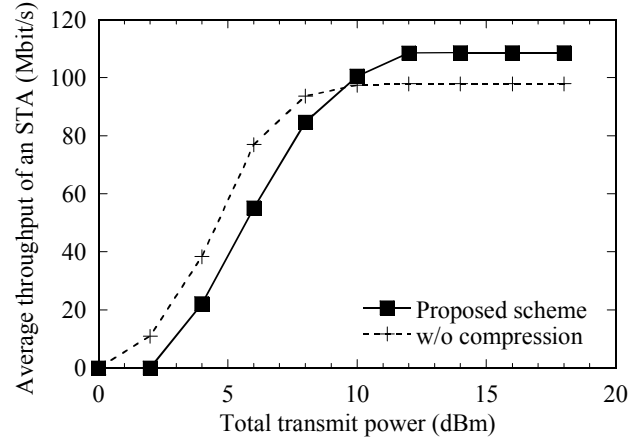


Fig. 8. Average throughput as a function of the total transmit power of a DL-MU-MIMO transceiver.